

# Identification, characterization and molecular phylogeny of U12-dependent introns in the *Arabidopsis thaliana* genome

Wei Zhu<sup>1,\*</sup> and Volker Brendel<sup>1,2</sup>

<sup>1</sup>Department of Zoology and Genetics and <sup>2</sup>Department of Statistics, Iowa State University, Ames, IA 50011-3260, USA

Received March 27, 2003; Revised and Accepted June 2, 2003

## ABSTRACT

**U12-dependent introns are spliced by the minor U12-type spliceosome and occur in a variety of eukaryotic organisms, including *Arabidopsis*. In this study, a set of putative U12-dependent introns was compiled from a large collection of cDNA/EST-confirmed introns in the *Arabidopsis thaliana* genome by means of high-throughput bioinformatic analysis combined with manual scrutiny. A total of 165 U12-type introns were identified based upon stringent criteria. This number of sequences well exceeds the total number of U12-type introns previously reported for plants and allows a more thorough statistical analysis of U12-type signals. Of particular note is the discovery that the distance between the branch site adenosine and the acceptor site ranges from 10 to 39 nt, significantly longer than the previously postulated limit of 21 bp. Further analysis indicates that, in addition to the spacing constraint, the sequence context of the potential acceptor site may have an important role in 3' splice site selection. Several alternative splicing events involving U12-type introns were also captured in this study, providing evidence that U12-dependent acceptor sites can also be recognized by the U2-type spliceosome. Furthermore, phylogenetic analysis suggests that both U12-type AT-AC and U12-type GT-AG introns occurred in Na<sup>+</sup>/H<sup>+</sup> antiporters in a progenitor of animals and plants.**

## INTRODUCTION

U12-dependent introns, initially discovered by Jackson (1) and Hall and Padgett (2), are a class of low-abundance introns which are spliced by a minor class (U12-dependent) spliceosome and are distributed in vertebrates, insects and plants (3). This rare class of introns is characterized by highly conserved consensus sequences / [AG]TATCCTT (where / denotes the exon end and [AG] indicates A or G) and TCCTTAAC at the donor and branch sites, respectively (2), in contrast to the

much more degenerate splice signals in the major class (U2 type) introns that are spliced by the U2-type spliceosome (reviewed in 4,5). Correspondingly, the U12-type spliceosome consists of specific U11, U12, U4atac and U6atac snRNAs that recognize the U12-type splice signals (6–8). In addition, U12-type introns lack a polypyrimidine tract between the branch site sequence (BSS) and the 3' splice site (3'ss). Despite these differences, the U12-type spliceosome resembles the conventional spliceosome in many ways (4). For instance, irrespective of the lack of sequence similarity, U11, U12, U4atac and U6atac snRNAs are likely to have roles in the U12-dependent spliceosome that are analogous to the roles of U1, U2, U4 and U6 snRNAs in the U2-dependent spliceosome, respectively. Recent experimental data proved that the stem-loop structure within the U6 snRNA can functionally substitute the U6atac snRNA stem-loop (9). Moreover, not only is U5 snRNA common in each of the two spliceosomes, but a growing number of auxiliary proteins have been confirmed to be shared by both spliceosomes (10–13). U12-type introns typically coexist with U2-type introns in alternate patterns in the same gene (3,14), and the splicing efficiency of U12-type introns can be promoted by splicing the flanking U2-type introns via the exon definition mechanism (15–17). U11/U12 di-snRNAs were found to bridge the 5' splice site (5'ss) and the BSS in the initial recognition of U12-type introns, suggesting that the mechanism of intron definition also functions in the splicing of minor introns (18).

The U12-dependent spliceosome may have coexisted with the conventional spliceosome in the common ancestor of higher eukaryotes (19). The fact that vertebrates and higher plants share conserved features in the functional regions of U6atac and U12 snRNAs also provides evidence indicating an early origin of the U12-dependent splicing system (20). The differences between the two splicing machineries imply that the two spliceosomes evolved parallel to each other in separate lineages and then merged prior to the divergence of the animal and plant kingdoms (3).

Another distinguishing feature of U12-type introns is that the distance between the branch site adenosine and the acceptor site (DistBA) is unusually short, between 10 and 20 bp (21), while the DistBA of the U2-type introns can be over 100 bp (22). It has also been experimentally confirmed that spacing mutations that generate a predicted DistBA <10 nt

\*To whom correspondence should be addressed at present address: NewLink Genetics, 2901 S. Loop Dr., Ames, IA 50010, USA. Tel: +1 515 296 0866; Fax: +1 515 296 5557; Email: wzhu@linkp.com

or >20 nt strongly activate cryptic 3'ss (23). As a result, Dietrich *et al.* (23) proposed a local diffusion model to explain acceptor site selection in U12-type introns.

The initial recognition of the U12-type introns arose from its non-canonical dinucleotide termini AT-AC (1), distinct from the conventional GT-AG intron borders. Further research indicated that GT-AG introns can be spliced by U12-type spliceosomes, and, conversely, AT-AC introns can be spliced by U2-type spliceosomes (24,25). Therefore, intron type cannot be simply determined by the dinucleotide termini. This raises the question of how to distinguish U12-type introns from U2-type introns. Based on conserved motifs of the donor site and the branch site in the U12-type introns, Burge *et al.* (3) designed a computer program, named U12Scan, to address the issue of the identification of U12-type introns and conducted a survey in a variety of species based on the GenBank gene structure annotation. Later, Levine and Durbin (14) adopted a slightly different strategy to recognize human U12-type introns. They predicted U12-type introns in the human genome first, and confirmed the hypothetical introns by expressed sequence data, requiring a 64 bp perfect match between a transcript sequence fragment and the 32 bp flanking sequences of a predicted U12-type intron in both directions. The latter approach did not suffer from the incompleteness or likely errors in the GenBank annotation, but has its own problems. For example, any U12-type intron flanked by exons shorter than 32 bp would not be located. In addition, both analyses restricted their search of DistBA within a short region of the introns consistent with the assumption that no U12-type introns have DistBAs shorter than 8 nt or longer than 21 nt.

In a recent study, we mapped 176 915 *Arabidopsis* ESTs on the *Arabidopsis* genome, and 45 U12-type introns were identified in the set of EST-confirmed introns (26). Here, we have undertaken a more sophisticated analysis including 26 961 *Arabidopsis* full-length cDNAs in addition to the EST set used in the previous study. A total of 165 distinct U12-type introns were identified, including 50 AT-AC introns, one AT-AA intron, one GT-AT intron and 113 GT-AG introns, comprising many more than the overall number of U12-type introns previously reported in plants. Our analysis indicates that *Arabidopsis* U12-type introns not only share similar features with *Arabidopsis* U2-type introns in intron length distribution and low GC content relative to the flanking exons, but they also share almost identical splice signals with U12-type introns from other species. One significant discovery is that five U12-type AT-AC introns and seven U12-type GT-AG introns have DistBAs longer than 21 nt, the longest observed distance being 35 nt. When further extending the BSS search region, another novel U12-type GT-AG intron was identified with a DistBA of 39 bp. The presumed 21 bp maximum limit appears incorrect, even though the distribution of DistBAs of the U12-type introns shows a peak at 12 nt. Several alternative splicing events involving U12-type introns were also found in this study and provide evidence that U12-dependent 3'ss could be recognized by the U2-type spliceosome. Analysis of the cases of alternative splicing combined with dinucleotide preference analysis also demonstrates that the sequence context of the potential acceptor site may also have an important role in 3'ss selection, in addition to the spacing constraint. Furthermore, phylogenetic analysis provided an example of conservation of U12-type introns (placement and

signals) throughout the plant and animal kingdoms in a family of Na<sup>+</sup>/H<sup>+</sup> antiporters, suggesting that both U12-type AT-AC and U12-type GT-AG introns occurred in the same gene in a progenitor of animals and plants.

## MATERIALS AND METHODS

### cDNA/EST-confirmed introns in the *Arabidopsis thaliana* genome

The *A. thaliana* genome sequence (release of August 20, 2002) was retrieved from GenBank (<http://www.ncbi.nih.gov/GenBank/>), with accession nos NC\_003070, NC\_003071, NC\_003074, NC\_003075 and NC\_003076 for the five chromosomes, respectively. *Arabidopsis* full-length cDNA sequences were also downloaded from GenBank (dated April 11, 2002), and *Arabidopsis* ESTs were downloaded from NCBI dbEST (<http://www.ncbi.nlm.nih.gov/dbEST/>) in December 2002. All 27 288 putative *Arabidopsis* proteins (data label: ATpep, version: July 25, 2002) were downloaded from The Institute of Genome Research ([ftp://ftp.tigr.org/pub/data/a\\_thaliana/ath1/SEQUENCES/ATH1.pep](ftp://ftp.tigr.org/pub/data/a_thaliana/ath1/SEQUENCES/ATH1.pep)), corresponding to the annotation of the same *Arabidopsis* genome release as the one used in this study.

A total of 26 961 full-length cDNAs and 176 915 ESTs were aligned with the *Arabidopsis* genome sequence using the GeneSeqer spliced alignment program (27) at high stringency in order to generate a reliable data set of *Arabidopsis* introns. The cDNA/EST-confirmed introns originated from the putative cognate spliced alignments with local similarity scores higher than 0.9 (26), and qualified introns were merged into a non-redundant intron set for subsequent analysis.

### Identification of *Arabidopsis* U12-type introns

The identification procedure used follows the procedure established by Burge *et al.* (3). A brief description is given in the following. First, weight matrices for the splice sites of U12- and U2-type introns were derived from subsets of the transcript-confirmed *Arabidopsis* introns. The U12-type intron subset consisted of 47 introns with AT-AC termini and two introns with AT-AA termini that display strong U12-type splice signals as previously identified in a variety of species (3,14). The weight matrices for the recognition of U12-type introns in the subsequent analysis were generated from this subset with the MEME program (28). In addition, 70 189 cDNA/EST-confirmed GT-AG introns which lack the U12-type consensus sequence ATCC in positions +3 to +6 relative to the 5'ss were utilized as a training set to construct the corresponding weight matrixes for U2-type introns. The probabilities of the intron-type signals were then computed as the products of the corresponding position-specific probabilities, based on the observed residue frequencies derived from the transcript-confirmed introns. The log-odds ratio of the score derived from the U12-type splice signals versus that from the U2-type splice signals was computed for the 5'ss and the BSS of all the transcript-confirmed introns included in the training sets. The log-odds ratios were further normalized by subtracting the sample mean and dividing by the corresponding standard deviation. The normalized scores are referred to as  $S_x$ , where  $x$  is d or b, denoting the donor site and the BSS, respectively. Then, introns with large values for both  $S_d$  and  $S_b$

were selected as U12-type introns [see Fig.1; also see fig. 2 in Burge *et al.* (3)]. Because one of the U12-type likely AT-AC introns in the training set has DistBA as long as 35 nt, we set the search region for the branch-site motif within the intron relative to the confirmed 3'ss corresponding to DistBA values in the range 6–35. The region [–5, +5] relative to the 5'ss was also scanned for possible ambiguities in assignment of the precise exon–intron junctions in cases where sequence repeats yield alternative spliced alignments. If necessary, such ambiguous cases were corrected manually to report the correct exon–intron borders.

### Gene duplications

3044 gene pairs were identified in a recent study of large-scale gene duplications in the *Arabidopsis* genome (29). The gene pairs and their related information were downloaded from <http://wolfe.gen.tcd.ie/athal/dup> and used to study the fate of the U12-type introns after gene duplication.

### Sequence alignment and phylogenetic tree construction

Homologous protein sequences were aligned by Clustal X (30) with default settings. The neighbor-joining trees were constructed based on the multiple alignments using MEGA2.1 (31), after removal of all columns in the alignment containing one or more gaps. The trees were based on the *p*-distance, which is the proportion of amino acid sites at which the two sequences compared are different. Confidence of the tree topology was assessed by a bootstrap test with 500 replicates.

### Dinucleotide relative abundance in the proximity of the acceptor site of U12-type introns

Let  $f_x$  and  $f_{xy}$  represent the frequency of the nucleotide  $x$  and the frequency of the dinucleotide  $xy$ , respectively. The dinucleotide relative abundance is defined as  $\rho_{xy} = f_{xy} / f_x f_y$ , as a common assessment of dinucleotide bias (32). Dinucleotide relative abundances were calculated for the region between 10 bp downstream of the branch site adenosine and 1 bp upstream of the 3'ss and also in the equally sized region immediately downstream of the 3'ss within the exon. As a control, dinucleotide relative abundances were also derived for the U2-type GT-AG intron sequences in the 10 bp regions immediately preceding and succeeding the 3' terminal dinucleotide. Hence, if the 5'-most AC downstream of the BSS is almost always selected as the 3'ss in U12-type AT-AC introns, the dinucleotide AC should be under-represented between the BSS and the 3'ss, that is,  $\rho_{AC}$  should be significantly smaller than 1.

## RESULTS

### Identification and characteristics of U12-dependent introns

There are 53 introns with AT-AC terminal dinucleotides and six introns with AT-AA termini in the non-redundant transcript-confirmed *Arabidopsis* intron set that were identified as candidate U12-type introns. Because of the absence of the typical U12-type motifs for both the donor site and the branch site, six AT-AC introns and four AT-AA introns were removed. The remaining 49 introns were utilized to build weight matrices for U12-type 5'ss and BSS. The weight

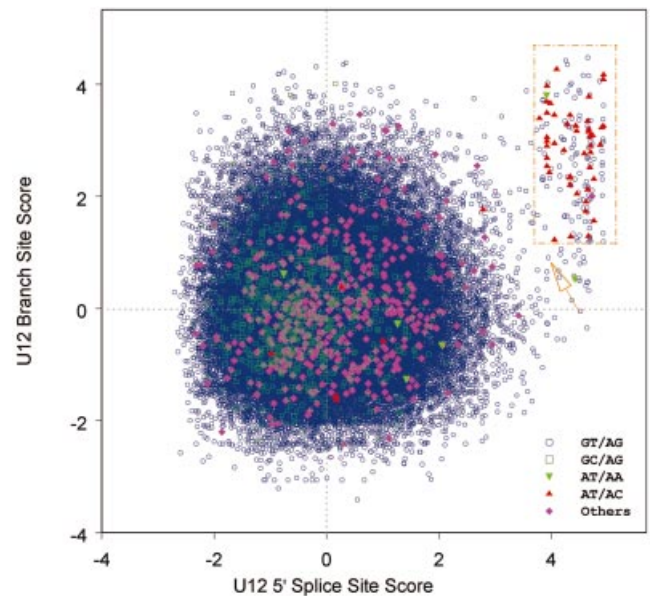


**Figure 1.** Identification of U12-type introns. Each transcript-confirmed intron is represented by a point at coordinates ( $S_d$ ,  $S_b$ ) where  $S_d$  and  $S_b$  are the statistical score for donor site and branch site, respectively. The yellow rectangle identifies introns that were empirically classified as U12 type. In addition, a yellow arrow indicates a U12-type likely GT-AG intron not included in the selection (see text for details).

matrices of U2-type introns 5'ss and BSS were also constructed based on transcript-confirmed U2-type GT-AG introns (see Materials and Methods). On the basis of the derived U12- and U2-type weight matrices, the pairs of the standardized scores ( $S_d$ ,  $S_b$ ) of 75 717 transcript-confirmed introns were computed (see Materials and Methods), projecting these introns into points in the two-dimensional plane (Fig. 1). As expected, the 49 U12-type like AT-AM (M represents A or C) introns from the training set map in the upper-right corner in the plot, accompanied by one GT-AT intron and hundreds of GT-AG introns. Consistent with the manual inspection mentioned above, six AT-AC introns and four AT-AA introns map close to the origin in the plane and are thus predicted to be spliced by the U2-type spliceosome. One AT-AC intron and one AT-AA intron included in the training data set have relatively low values in either  $S_d$  or  $S_b$  when compared with the other 47 U12-type AT-AM introns. We conservatively excluded these two introns from further analysis. The remaining 47 AT-AM introns were selected as authentic U12-type introns for reference. Because there is not an obvious cluster to separate the putative U12-type introns from U2-type introns, the determinant of U12-type introns versus U2-type introns was empirically defined with respect to the standardized scores of the 47 introns in the reference set, such that the U12-type intron should satisfy the condition that  $S_d$  and  $S_b$  are no less than the minimum value of  $S_d$  ( $= 3.79$ ) and  $S_b$  ( $= 1.23$ ) from the 47 U12-type AT-AM introns, respectively. The selected introns roughly enclosed by the yellow rectangle in Figure 1 include 110 GT-AG introns, 46 AT-AC introns, one AT-AA intron and one GT-AT intron.

All 158 predicted U12-type introns and related information are listed in a table provided as Supplementary Material,

**Table 1.** U12-type introns involved in alternative splicing

	ID	Chromosome	Location Start	End	Termini	DistBA	Evidence	Gene ID	Description
Alternative acceptor site	40	2	11193817	11193727	gt_ag	27	2	At2g26430	Putative cyclin
	41	2	11193817	11193734	gt_ag	20	11		
	68	3	4388199	4387910	gt_ag	26	1	At3g13460	Unknown protein
	69	3	4388199	4387919	gt_ag	17	9		
	83	3	19360482	19360367	gt_ag	14	5	At3g52180	Putative protein
	84	3	19360482	19360395	gt_ag	?	1		
	102	4	5098265	5098368	gt_at	10	1	At4g09720	GTP-binding protein, putative
Alternative donor site	103	4	5098265	5098373	gt_ag	15	2		
	58	2	18375661	18375494	gt_ag	13	2	At2g44680	Putative casein kinase II beta subunit
	NA	2	18375664	18375494	gc_ag	?	6		
	90	3	22278983	22278836	gt_ag	14	2	At3g60250	Regulatory subunit of protein kinase CK2
Exon skipping	NA	3	22278986	22278836	gc_ag	?	1		
	18	1	17781408	17781268	gt_ag	22	1	At1g49160	Putative serine/threonine protein kinase
	NA	1	17781576	17781268	gt_ag	?	2		

For each entry the columns list an ID matching the *Arabidopsis* U12-type intron ID in the table provided as Supplementary Material (IDs for U2-type intron are not available; NA), the genomic location, the intron termini, the distance between the presumptive branch site and the acceptor site (DistBA; where '?' denotes uncertain distance), the number of independent transcript sequences supporting the intron, and the corresponding gene name and description.

together with another four U12-type AT-AC introns and three U12-type GT-AG introns identified by non-cognate transcripts described in the next section. As shown in Table 1, there are four U12-type GT-AG introns that are alternatively spliced with cryptic acceptor sites in the proximity of the normal 3'ss, which leads to ambiguity in the determination of DistBA in these cases. Thus, the analysis of the DistBA distribution was based on the remaining 157 distinct introns (51 AT-AM introns and 106 GT-AG introns) after excluding the four pairs of introns involved in alternative splicing (including seven GT-AG introns and one GT-AT intron; also see Table 1). As shown in Figure 2, the DistBA distribution of the U12-type AT-AM introns seems similar to that of the U12-type GT-AG introns. In particular, both distributions have the mode at 12 nt, and in both sets the shortest DistBA is 11 nt. Interestingly, 12 U12-type introns (five AT-AC introns and seven GT-AG introns) have distances longer than 21 nt, the maximum distance previously reported (14,23). To be conservative in assessing the authenticity of the U12-type introns in this study, the introns with long DistBA (>21 bp) were left out in the subsequent analysis of the sequence characteristics of U12-type introns.

Thus, 46 U12-type AT-AM and 99 U12-type GT-AG introns comprise the set for further analysis. The *Arabidopsis* U12-dependent splice signals display a similar base composition to that of previously identified U12-type introns from various species (3). There is no significant difference in the length distribution between the U12-type introns and U2-type introns in *Arabidopsis* (Fig. 3), in contrast to the reported lack of short U12-type introns relative to U2-type introns in human (14). Furthermore, plant introns are characterized by low GC content when compared with the flanking exons (33), and our analysis shows that U12-type introns have this trait in common with the U2-type introns in *Arabidopsis* (data not shown).

### Gene duplications and molecular phylogeny analysis

A recent study suggested that the *Arabidopsis* genome has undergone at least two large-scale duplications (29). The authors identified 3044 gene pairs divided into 91 chromosomal blocks and concluded that one event was a recent

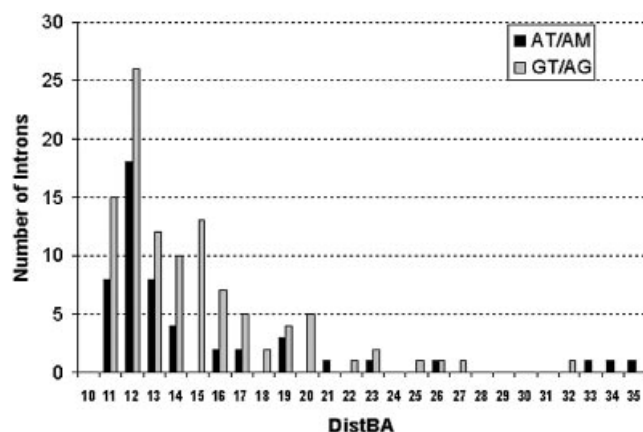


**Figure 2.** Histogram of branch site to acceptor site distances (DistBA) of U12-type introns. The distances were compiled from 51 U12-type AT-AC or AT-AA introns (black bars) and 106 U12-type GT-AG introns (gray bars) listed in Supplementary Material. Note that 12 U12-type introns (five AT-AC introns and seven GT-AG introns) have branch site to 3'ss distances that are longer than 21 bp.

polyploidy which occurred 24–40 millions years ago (mya) and that the other event was an older one which happened after the monocot/dicot split. We found that among this set there are 24 gene pairs that have at least one U12-type intron in one or the other gene (Table 2). Based on our stringent criteria, the candidate U12-type introns are highly likely to be authentic U12-type introns. We cannot be sure, however, that the remaining transcript-confirmed introns are necessarily spliced by the major spliceosome, and, moreover, lack of transcript evidence may cause some U12-type introns in the duplicated gene set to remain undetected. In only two of the 24 gene pairs, the U12-type intron cannot be matched up with an intron in the paralog, reflecting an instance of intron loss or gain. Two of the gene pairs conserve a U12-type AT-AC intron, and six gene pairs conserve a U12-type GT-AG intron. Manual inspection led us to clarify three additional introns each as conserved AT-AC and GT-AG U12-type introns, respectively. In the remaining eight gene pairs there are five cases of

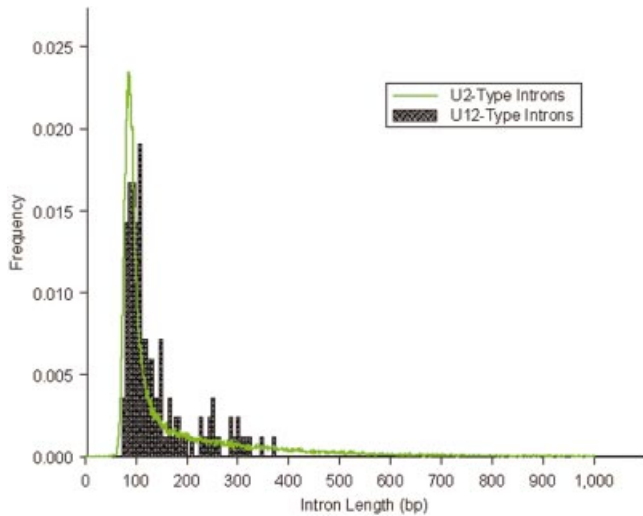


**Figure 3.** Length distribution of the U12- and U2-type introns. The histogram for the U2-type introns was derived from 70 189 transcript-confirmed *Arabidopsis* introns (plotted in green line). The histogram for U12-type introns (filled column) is based on 145 sequences.

uncertain GT-AG U12-type conservation (one of the introns in each pair having below-threshold  $S_d$  and  $S_b$  scores), two possible conversions of U12-type GT-AG introns to U2-type GT-AG introns (occurring in the only two gene pairs derived from the ancient large-scale gene duplications), and one case of a GT-AG/AT-AC U12-type pair. Excluding the five ambiguous cases, U12-type introns were stably conserved in 15 out of the remaining 19 pairs since the onset of gene divergence ~24–40 mya (29). Thus, U12-type introns seem to be very stable in recent gene duplications, but are likely to be converted into U2-type introns in the long run.

Because occasional (random) gene duplications occur in addition to the large-scale segmental genome duplications, we searched all the genes containing U12-type AT-AM introns against ATpep using BLASTP (34) and identified additional duplicated genes. This resulted in the detection of another novel U12-type AT-AC intron in the gene At1g76170, supported by spliced alignment of the non-cognate EST gi:23303104 from its paralogous gene At2g44270. The BLAST search also revealed more cases of the conservation of U12-type introns. The gene At1g79610, which encodes a low abundance  $\text{Na}^+/\text{H}^+$  antiporter (AtNHX5) active in shoots and roots in *Arabidopsis* (35), contains a total of two U12-type AT-AC introns (intron 3 and 10), one U12-type GT-AG intron (intron 15) and 18 U2-type introns (see Supplementary Material for detailed descriptions of the U12-type introns). AtNHX5 shares its highly conserved sequence and gene structure with another family member, AtNHX6 (from gene At1g54370), which has two matching U12-type AT-AC introns (introns 3 and 10; listed in Supplementary Material). The intron type of the counterpart (intron 15) in AtNHX6 of the U12 GT-AG intron of AtNHX5 is uncertain, because the intron has a strong U12-dependent donor site but a relatively weak U12-dependent branch signal (TTCATGAC;  $S_b = 0.89$ ) with an 11 bp DistBA (indicated by the yellow hollow arrow in Fig. 1). However, the intron has a strong U12-dependent branch site signal (TCCTTGAC;  $S_b = 3.40$ ) with a 39 bp

**Table 2.** The fate of U12-type introns after large-scale segmental duplications in the *Arabidopsis* genome

Block ID	Age	Gene1	Gene2	Ks
0305290000580	recent	At3g44750	At5g22650	1.0943
0505065400320	recent	At5g08430	At5g23480	0.9469
0203257711080	recent	At2g47650	At3g62830	0.8186
0305033201380	recent	At3g05700	At5g26990	0.9514
0305052001580	recent	At3g06760	At5g49230	0.9555
0305328300280	recent	At3g49410	At5g24450	0.6644
0305331801560	recent	At3g51460	At5g66020	0.6112
0103319703610	recent	At1g49160	At3g18750	1.2050
0204107902160	recent	At2g20230	At4g28770	1.0095
0203257711080	recent	At2g41740	At3g57410	0.5008
0203257711080	recent	At2g44680	At3g60250	0.7847
0305000103160	recent	At3g03340	At5g17440	0.6363
0505069001350	recent	At5g10060	At5g65180	0.9116
0102031203980	recent	At1g06890	At2g30460	0.7299
0104000102440	recent	At1g02890	At4g02480	0.5794
0505065400320	recent	At5g08390	At5g23430	0.5045
0104000102440	recent	At1g01100	At4g00810	3.7616
0104000102440	recent	At1g01050	At4g01480	0.7543
0203257711080	recent	At2g44150	At3g59960	0.9011
0204153002470	recent	At2g25310	At4g32130	0.6263
0405128403640	recent	At4g17640	At5g47080	0.8517
0204341201650	old	At2g46660	At4g01480	1.8172
0405237901400	old	At4g30160	At5g57320	1.6217
0104000102440	recent	At1g02750	At4g02200	1.1220

Listed are all gene pairs derived from large-scale segmental genome duplications for which at least one gene contains a U12-type intron. For each gene pair, the columns give the block identifier (ID), age and synonymous substitution rate (Ks) according to Blanc *et al.* (29); data downloaded from <http://wolfe.gen.tcd.ie/athal/dup>. U12-type introns with AT-AC or GT-AG termini are indicated by green or yellow shading, respectively. Olive and orange shading indicate AT-AC and GT-AG U12-type introns identified by comparison with the duplicated gene (rather than primary EST or cDNA evidence). In the gene pairs listed in the first two rows, one of the genes (cells not shaded) does not contain an intron in equivalent position. Gray shading indicates GT-AG introns with weak U12-type splice signals preventing unambiguous classification of these introns as U12 or U2 type. Highly likely U2-type introns are identified by red shading.

DistBA, whereas the branch site of the corresponding U12-type GT-AG intron in AtNHX5 has a DistBA of 32 bp. Whether the intron is an authentic U12-type intron and whether the high score branch site is functional *in vivo* will have to be determined by experimental methods. It would be the longest DistBA for the U12-type introns identified to date, if confirmed. There are four other members of  $\text{Na}^+/\text{H}^+$  antiporter in *Arabidopsis* (AtNHX1–4). AtNHX5 and AtNHX6 have more sequence similarity with the human  $\text{Na}^+/\text{H}^+$  exchangers HsNHE6 and HsNHE7 (Fig. 4; also see fig. 2 in Yokoi *et al.* (35)). Interestingly, there are two U12-type GT-AG introns and one U12-type AT-AC intron reported in HsNHE6 (14). The Ensembl annotation indicates that the two corresponding U12-type GT-AG introns also exist in HsNHE7 ([http://www.ensembl.org/Homo\\_sapiens/exonview?transcript=ENST00000163256&db=core](http://www.ensembl.org/Homo_sapiens/exonview?transcript=ENST00000163256&db=core)). The annotation also displays an U2-type GT-AG intron near the location of the corresponding U12-type AT-AC intron in the locus of HsNHE7 (see Fig. 4A). However, this intron has intact U12-type splice site sequences, suggesting that the U12-type AT-AC introns may still be functional in HsNHE7 (Fig. 4B). Additionally, there are no U12-type introns in AtNHX1–4, which actually have almost completely different gene

structures compared with AtNHX5–6. As shown in Figure 4A–C, the U12-type AT-AC intron and one of U12-type GT-AG introns have conserved locations between AtNHX5–6 and HsNHE6–7. With respect to the neighbor-joining tree of Na<sup>+</sup>/H<sup>+</sup> antiporters from *Arabidopsis*, human, rice, *Escherichia coli*, yeast and other species [Fig. 4D; also see fig. 2 in Yokoi *et al.* (35)], we may infer that the appearance of the U12-type introns is dated prior to the divergence of AtNHX5–6 from HsNHE6–7, but after the divergence of AtNHX5–6 and AtNHX1–4.

The genes At1g02750, At1g56280, At3g05700, At3g06760, At4g02200, At5g26990 and At5g49230 that encode proteins

thought to be drought induced, all have one U12-type AT-AC intron in the same location. The only exception is the gene At4g02200, which has a U12-type GT-AG intron instead. After correcting annotation errors based on the transcript sequence data, the protein sequences of the seven genes and a homologous gene from rice (accession no. AAO33770) were aligned by Clustal X [Fig. 5A; for Clustal X see Jeanmougin *et al.* (30)] and a neighbor-joining tree was constructed based on the multiple alignment using MEGA2.1 [Fig. 5B; for MEGA2.1 see Kumar *et al.* (31)]. Detailed analysis indicates that the gene structures are highly conserved among the seven *Arabidopsis* genes and the rice gene. The identified U12-type

**A**

		370	380	390	400	410	420	
AtNHX1	217	YLFLLSTLLGAATGLISAYVIK	KKLYFGRHSTD-REVALMMLMAYLSYMLAELFD-LSGIL	274				
AtNHX2	219	YLFLLSTGLG VATGLISAYVIK	KKLYFGRHSTD-REVALMMLMAYLSYMLAELFA-LSGIL	276				
AgNHX1	221	YLFIASTILGAFTGLLSAYI	IKKLYFGRHSTD-REVALMMLMAYLSYMLAELFY-LSGIL	278				
OsNHX1	219	YLFLLSSTFLGVFAGLLSAYI	IKKLYIGRHSST-REVALMMLMAYLSYMLAELLD-LSGIL	276				
InNHX1	219	YLFLLSSTFLGVGIGLLCAYI	IKKLYFGRHSTD-REVALMMLMSYLSYMLAELFY-LSGIL	276				
AtNHX3	220	YLFILSTALGVAAGLLSAFVI	KKLYIGRHSST-REVALMMLLAYSMLAELFH-LSSIL	277				
AtNHX4	217	YLFSTSTLLGIGVGLITSEV	LTKLYFGRHSST-RELAIMVLMAYLSYMLAELFS-LSGIL	274				
HsNHE6	297	GIFSGSFAMGAATGVVTA	LVTKFT--KLREFQLEETGLFFLMSWSTFLLAEAWG-FTGVV	353				
HsNHE7	329	GIFSGSFTMGAVTGVN-ANV	TKFT--KLHCFPLELETALFFLMSWSTFLLAEACG-FTGVV	384				
AtNHX5	221	ETFAGSMSAGVGVGFTSAIL	LFKYAGLDTENLQNLECCFLVLFYFYSYMLAEGVG-LSGIV	279				
AtNHX6	225	ETFVGSMSAGVGVGFTSAIL	LFKYAGLDVDNLQNLECCFLVLFYFYSYMLAEGLS-LSGIV	283				
HsNHE1	300	VVALGGVLVGVVYGVIAAFT	SRFT---SHIRVIEPLFVFLYSYMLAELFH-LSGIM	354				
HsNHE2	280	VVGIGGVVIGIFLGFIAAFT	TRFT---HNIRVIEPLFVFLYSYLSYTAEMFH-LSGIM	334				
HsNHE3	256	VVSLGGTLVGVVFAFLLSLV	TRFT---KHVRIIEPGFVFIISYLSYLTSEMLS-LSAIL	310				
ScNHX1	262	MTFSVLLIGVLIGLIVALLK	HKT--HIRRYPQIESCLILLIAYESYFNSGCH-MSGIV	318				
AtSOS1	231	KVALGAVGIGLAFGIASV	IWLKFI---NDTVIEITLTIASVFANYTAQEWAGASGVL	286				
EcNhaA	183	SLGVAVAIAVLAVLNL	CGARRT---VYILVGVVLTAVLKSQVHATL	228				
EcNhaB	211	ALGGVMTMVEPQNLI	IAKAAGWHFGDFFLRMS PVTVPVLCGLLTCLLVEKLR-WFGYG	269				

**B**

actggtgtt|gtgactgctctaataatccttttgt.....tacctggagacagggtccttgacag|aatgccaacgtgactaag  
T G V V T A L N A N V T K

**C**

		490	500	510	520	530	540	
AtNHX1	335	PGTSIAVSSILMGLVMVG	GRAAFVFPPLSFLSNLAKKNQ-----SEKINFNM	379				
AtNHX2	337	PGTSVAVSSILMGLVMLG	RAAFVFPPLSFLSNLAKKHQ-----SEKISIKQ	381				
AgNHX1	339	PGISVAVSSILLGLVMVG	RAAFVFPPLSWLMNFAKKSQ-----SEKVTFNQ	383				
OsNHX1	337	PGKISIGISSILLGLVLIG	RAAFVFPPLSFLSNLTKKAP-----NEKITWRQ	381				
InNHX1	337	QGLSVAVSSILVGLILV	GRAAFVFPPLSFLSNLAKKNS-----SDKISFRQ	381				
AtNHX3	338	PGQSIGVSSILLGLILLG	RAAFVFPPLSFLSNLTKSSP-----DEKIDLKK	382				
AtNHX4	335	FGGTLGVSGVITLVLLG	RAAFVFPPLSVLTFNFMNRHTER-----NESITFKH	381				
HsNHE6	410	----PTFVVGAFVAIFL	GRAANIYPLSLLNLGR--R-----SKIGSNF	448				
HsNHE7	441	----PIFIIGAFVAIFL	GRAAHIYPLSFFNLGR--R-----HKIGWNF	479				
AtNHX5	336	----VGFIIFSILFIG	VARAVNVFGCAYLVNLFQEN-----QKIPMKH	376				
AtNHX6	340	----LGFIFFSILFIV	IARAANVFGCGYLVNLARPAH-----RKIPMTH	380				
HsNHE1	410	----WTFVISTLLFCL	IARVGLVGLTWFINKFRIVK-----LTPKD	448				
HsNHE2	390	----WAFVCFTLAFCL	MWRALGVFVLTQVINRFTIP-----LTFKD	428				
HsNHE3	367	----TAFVLLTLVFI	SVYRAIGVVLTQVWLLNRYRMVQ-----LEPID	405				
ScNHX1	375	----PLLIIVAAISIC	VARWCADFPLSQFVNWIRVKTIRSMSGITGENISVPDEIPYNY	431				
AtSOS1	347	QGNSWRFLFLLYVYI	QLSRVVVGVLYPLLCFRG-----YGLDWKE	387				
EcNhaA	285	----SILPLGIIAGLL	IGKPLGISLFCWLALRLKLAH-----LPEGTTY	325				
EcNhaB	326	----VIILATSLT	GVTDDEHAIGKAFTESLPFTALLT-----VFFSV	363				

introns are all in coding phase 0 (i.e. splitting two neighboring codons) and the same position starting after the conserved lysine (K103, highlighted in green in Fig. 5A), where an U2-type GT-AG intron is located in the rice homolog. We were particularly interested in this example to find out how the U12-type AT-AC intron switches to the U12-type GT-AG intron in the gene At4g02200 since the divergence from the gene At1g02750. The multiple alignment of At4g02200, At3g05700 and At1g02750 suggests that the conversion was probably initiated by the mutation of the 5' terminal AT to GT, with subsequent activation of an AG downstream of the original acceptor site as the canonical 3'ss (Fig. 5C).

In total, non-cognate transcripts helped to identify four U12-type AT-AC introns and three GT-AG introns in this extended search. High conservation of the U12-type introns among paralogous genes was also observed in previous studies (3,14).

### Alternative splicing

Seven cases of alternative splicing events related with U12-type introns were captured in this analysis (listed in Table 1).

Four of the cases involve alternatively activated cryptic acceptor sites in the proximity of the normal splice sites. In detail, the GT-AG U12-type introns in the genes At2g26430 and At3g13460 both have minor isoforms utilizing CAG/, 7 and 9 nt downstream of the cognate acceptor site TAG/, respectively. This suggests that the distal AG with the favored sequence motif CAG/ may compete with the first AG downstream of the BSS in 3'ss selection of U12-type GT-AG introns. The 'leaky' scan revealed by these two alternative splicing events also implies that the spacing constraint in the 3'ss selection may not be as strong as previously assumed. Differing from the previous two examples, the U12-type GT-AG intron in At3g52180 has a cryptic acceptor site 28 nt upstream of the wild-type acceptor and 14 bp preceding the normal U12-dependent branch site. Motif search for U12-type branch site signals suggests the sequence TCCTTCGC as the most likely alternative branch site signal ( $S_b = 1.66$ ; with DistBA 28 bp, but G replacing the usual A) or GTTTTCAC ( $S_b = -1.31$ ; with DistBA 38 bp, unusually long). An alternative explanation is that the transcript isoform is spliced by the U2-type spliceosome rather than the minor

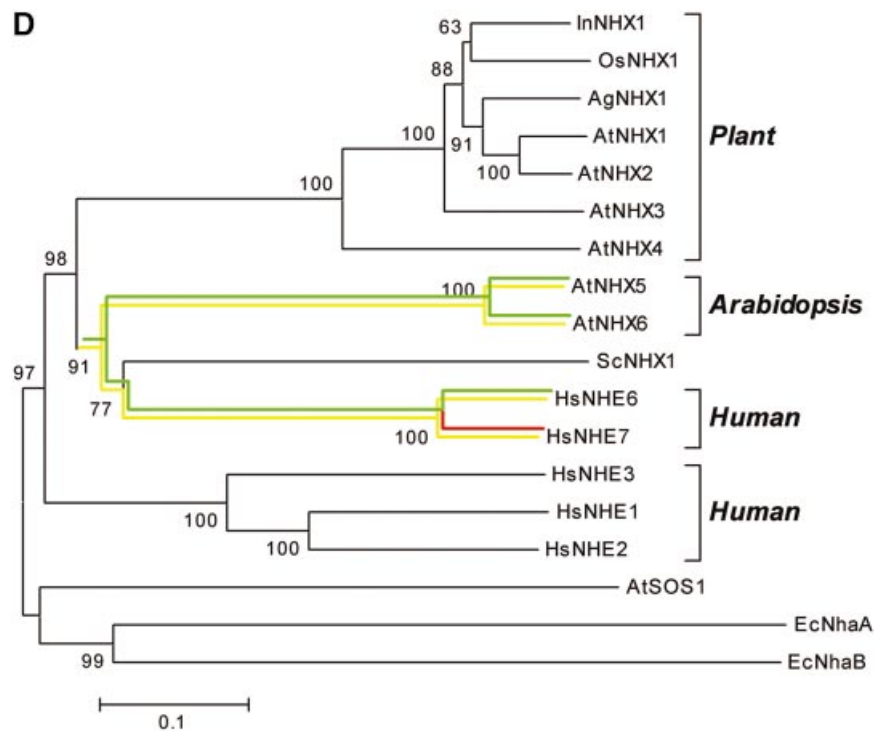


**Figure 4.** (Opposite and above) Analysis of  $\text{Na}^+/\text{H}^+$  antiporters. The sources of the  $\text{Na}^+/\text{H}^+$  antiporter protein sequences are as follows (GenBank accession nos in parentheses): AtNHX1 (AAD16946), AtNHX2 (AAM08403), AtNHX3, (AAO41905), AtNHX4 (AAM08405), AtNHX5 (AAM08406), AtNHX6 (AAM08407) and AtSOS1 (AAF76139) from *A.thaliana*; InNHX1 (BAB60899) from *Ipomoea nil*; OsNHX1 (BAA83337) from rice; AgNHX1 (BAB11940) from *Atriplex gmelini*; ScNHX1 (NP\_010744) from yeast; HsNHE1 (P19634), HsNHE2 (AAD41635), HsNHE3 (P48764), HsNHE6 (Q92581) and HsNHE7 (NP\_115980) from human; EcNhaA (P13738) and EcNhaB (P27377) from *E.coli*. (A) The region [361, 420] of the multiple alignment of the  $\text{Na}^+/\text{H}^+$  antiporters. Residues in each column of the alignments are shaded in black or gray if >70% of residues in the column are identical or similar. A phase-0 (i.e. between codons) U12-type AT-AC intron is marked by an upside down green triangle for AtNHX5, AtNHX6 and HsNHE6. Correspondingly, a phase-0 U2-type GT-AG intron is marked by a red triangle in HsNHE7. (B) The nucleotide sequences around the termini of the U2-type GT-AG intron marked by the red triangle in HsNHE7 in (A) (where | represents an exon-intron junction) and the sequence of the translation product. The intact U12-type splice signals are marked by shading. The potential U12-dependent splicing would replace the NAN tripeptide in the translation of the transcript resulting from U2-type splicing with the tetrapeptide VTAL, equal to the sequence in HsNHE6. (C) The region [481, 540] of the multiple alignment of the  $\text{Na}^+/\text{H}^+$  antiporters. A phase-0 U12-type GT-AG intron is marked by an upside down yellow triangle for AtNHX5, AtNHX6, HsNHE6 and HsNHE7. (D) Neighbor-joining tree derived from the multiple alignment of the  $\text{Na}^+/\text{H}^+$  antiporters using MEGA2 (31). The numbers on the tree branches are bootstrap values, and branch lengths are proportional to the pairwise  $p$ -distances as indicated by the scale bar in the lower left (see Materials and Methods for details). The branches are colored green, yellow and red corresponding to the occurrences of U12-type AT-AC, U12-type GT-AG and U2-type GT-AG introns, respectively.

spliceosome. The U12-type intron in the gene At4g09720 has a cryptic and unusual acceptor site AT/ (5 nt upstream of the cognate 3'ss) with a DistBA of 10 nt, which is the shortest DistBA found in this study.

Of the remaining three instances of alternative splicing listed in Table 1, one involves a U12-dependent donor site /GT (supported by two sequenced transcripts) 3 nt downstream of the dominant donor site /GC (supported by six sequenced transcripts) in the gene At2g44680. Further analysis revealed that the U12-type GT-AG intron in the paralogous gene At3g60250 is also alternatively spliced with a similar pattern. Interestingly, based on the few transcripts sampled, the major isoform for gene At3g60250 is the U12-type 5'ss /GT instead of the U2-type 5'ss /GC for gene At2g44680. The third example is an exon skipping event in the gene At1g49160, a putative serine/threonine protein kinase. The U12-type GT-AG intron in At1g49160 is alternatively spliced using the

donor site of the upstream U2-type GT-AG intron. In all three examples, the alternative transcripts pair the U12-type 3'ss with an U2-type donor site, suggesting that a U12-type 3'ss can also be recognized by the major spliceosome. These examples also reveal a potential pathway for the conversion from U12-type GT-AG introns to U2-type introns via alternatively activating a cryptic U2-type 5'ss that subsequently becomes fixated. By EST evidence, retention of the U12-type AT-AC intron was observed in the genes At1g73350 and At5g63700. Intron retention may be a step preceding the loss of the U12-type AT-AC introns.

### Selection of the acceptor site of U12-type introns

In our large-scale analysis on the *Arabidopsis* genome, we identified only four combinations of terminal dinucleotides for U12-type introns, with the vast majority GT-AG and AT-AC and only one U12-type AT-AA intron and one U12-type

**A**

		10	20	30	40	50	60	
At1g02750	1	MEDDMVCSSSSGSSRSYRSETAAKYQSGPYQD-LEEFEEVDDDI AVEYPCPFCA SDYDLV						59
At4g02200	1	MEDLLGICGFDSSKKYRLEELAKYQSGSCIE-FED----DDEMAVDYPCPFCA SDYDLV						55
At3g06760	1	MDSN-WINCPSVFFSSSSSSRRCCQSRDL YLGGYEDLEGEDDL KA E F I C P F C A E D F D I V						59
At5g49230	1	MDSNSWINC P V F S S S P S S - R R Y Q S R S D L Y L G - - - - D V E G E D D L K A E F M C P F C A D E F D I V						55
At3g05700	1	MDS DS W S D R - - L A S A T R R Y Q L A F P S R S D T F L G - - F E E I D G E E E F R E E F A C P F C S D Y R D I V						56
At5g26990	1	MDS DS W S D R - - L A S A S R R Y Q L D F L S R S D N F L G - - F E E I E G E D D F R E E Y A C P F C S D Y R D I V						56
At1g56280	1	MDAD-----SKRFLATLRSRSEMLMG--FE E I D G D D D F Q E E F A C P F C A E S Y D I I						47
AA033770(rice)	1	-----MEVEAHHGFLPPAAGRQHLYGHPHYQLSGDDEWWEYIPCFPCYIEVEVP						49
		70	80	90	100	110	120	
At1g02750	60	ELCHHIDEERHEANNGICPVCSKRVKMHVVDHITSHRDVLS EQEKMSYREDPYLSDK						119
At4g02200	56	ELCHHIDEERHOLDANNGICPVCSRRVKMHVVDHITTOHRDVFRLYKDESYS AFSPGTRK						115
At3g06760	60	GLCCHIDEERPVEAKNGVCPVCTKRVGLDIVGHITTOHANFFVQRRLRRGGYSTYL						119
At5g49230	56	GLCCHIDVNEPVEAKNGVCPVCTKRVGLDIVGHITTOHGNVFRVQRRLRRGGYSTYL						115
At3g05700	57	SLCCHIDEERPMEAKNGVCPVCAVRVGVDLVAHITLOHANIFMHRKRKRPRGGYSTLS						116
At5g26990	57	SLCCHIDEERPMDAKNGVCPVCAVRVSSDMI AHITLOHANMFRVTRKRKSRGGAGSMLS						116
At1g56280	48	GLCCHIDEERTLESKNVCPVCSLKVGVDIVAHITLHGGSLFLQRKRKRKSGTMTLS						107
AA033770(rice)	50	FLCDHLCEBEFCFDMKNVCPVCAADNLDKDTDEHFRVQSHLLR--RRKSSSFCKPSSAA						107
		130	140	150	160	170	180	
At1g02750	120	YLQPHLDEL-----PPSMNHQHPSKHVSDQFLSFINNSALFNQTKLVLPDSS----						167
At4g02200	116	YLQSLIDEP-----LSTN----HTSKSVLDPLLSFIYNPPSPKKS KLVQPDSSSEAS						163
At3g06760	120	ALKKELREANLQSL LGSSS---FTSSTNIDSDPLLSF MFN-SFSVNQSANKSATPVTV						175
At5g49230	116	TLKKELREANLQS-LGSSST---FIPSSNIDSDPLLSF MFK-PP-----SAIPITE						162
At3g05700	117	ILRREFPDGNFQSLF GSSS C I V S S S S S S N V A A D P L L S S F I ---S P I A D G F F T T E S C I S A E						173
At5g26990	117	ILKREFPDGNFQSLFEGTSRAVSSSSAS-IAADPLLS SFI---SFMADDF F I E S S L C A D						172
At1g56280	108	LLRRELREGDLQRL LGFTSR--NGSVASSVTPDPLLS SFI---SETR-----SQSSPAPR						157
AA033770(rice)	108	ADKGSYEEDS----YFEAPSHCMGRPA PDSSP D P L L S C F I C ---C S L A P P V D S P R R S E A D A						161
		190	200	210	220	230		
At1g02750	168	VEDKNPIKDSAAKEGTSSCPLSDSDKLERAKKCEFVQGLLSSAMFDDCEDSSSE						221
At4g02200	164	MEDNSLIRDS-TEKDWESPSPS DTELLERAKKREFVQGLLSSAIFDHIYNF--						214
At3g06760	176	GNAATKVS IKESLKRDIQEAPLSGED-CERAKKSEFVRGLLSTMLEDDF----						224
At5g49230	163	GDSVAQVSPKDTSKSKIQQESFSNED-CERAKKSKFVRGLLSTMLEDKF----						211
At3g05700	174	TGPVKKTTIQCLPEQNAKKTSLAEDHKQRLKRSEFVRELLSSTILDDSL----						223
At5g26990	173	TSSAKKTLNQS L P E R N V E K Q S L S A E D H R E R L K Q S E F V Q G L S S M I L E D G L - - - -						222
At1g56280	158	QTKNVSEDKIERKRQVFISPVSLKDRERRHKSEFVQRLSSAIFDEV----						206
AA033770(rice)	162	EGHGSSSSDDQKRREQGVMDASKEELEERLQRIEFVKQLMTT IAY-----						208



GT-AT intron (the latter belonging to a splicing isoform as mentioned above). It seems that the selection of the 3' terminal dinucleotides of U12-type introns is highly correlated with the selection of the 5' terminal dinucleotides of U12-type introns, that is /GT is typically matched with AG/, and /AT is paired with AC/ or AA/ occasionally. In order to probe whether the scanning model is applicable in the selection of U12-type 3'ss, we computed the dinucleotide preferences in the region around the U12-type acceptor site (see Materials and Methods; Fig. 6). The results indicate that all dinucleotides starting with adenosine are under-represented upstream of the U12-dependent acceptor site. Further analysis revealed that there are six AC occurrences between the BSS and 3'ss in the total 51 AT-AM introns. All six AC are located in introns with DistBA < 18 nt, and in each case the AC occurs immediately upstream of the 3'ss AC/. In none of these cases is the first AC preceded by a C, so that these sites conform to the consensus pattern [AGT]ACAC/. Thus, CAC/ seems to be strongly preferred as the acceptor site of U12-type AT-AC introns. This suggests that the selection of the U12-dependent acceptor site does not follow a simple scanning mechanism that selects the first AC following the branch site as the acceptor site. Rather, the sequence surrounding the 3'ss also plays an important role in the selection of U12-dependent acceptor sites. In this context, the five U12-type AT-AC introns with DistBA larger than 21 nt all have CAC/ as the acceptor site, further indicating the importance of the surrounding sequence in the selection of U12-type 3'ss.

AG is strongly avoided in the proximal region prior to the acceptor site in either of the two classes of introns. Excluding the U12-type introns involved in alternative splicing, only one dinucleotide AG was found immediately prior to the cognate 3'ss CAG/ (in gene At4g02200). It seems that the scan model may be more applicable to the U12-type GT-AG introns than to the U12-type AT-AC introns.

**DISCUSSION**

**Identification of U12-type introns**

Using a computational approach that largely follows the procedure proposed by Burge *et al.* (3), we identified a total of 165 U12-type introns in the *Arabidopsis* genome, including 50 AT-AC introns, one AT-AA intron, 113 GT-AG introns and one GT-AT intron. A slight difference in our approach is the definition of the test criterion for intron-type classification. Burge *et al.* used as the test statistics  $t = S_b^2 + S_d^2 > 20$ , where  $S_b$  and  $S_d$  are normalized log-odds ratios discriminating U12-type introns against U2-type introns by branch and donor site characteristics, respectively. This criterion implies that an intron with a strong U12-dependent donor site signal (i.e.  $S_d > \sqrt{20} \approx 4.47$ ) should still be spliced by the U12-type spliceosome, in spite of a possibly weak branch site signal (and vice versa). Experimental evidence indicated that the donor and branch sites interact simultaneously in a U11/U12 di-snRNA complex at the step of initial recognition of the U12-type intron by the minor spliceosome (18). Other studies showed that normal U12-dependent intron splicing can be abolished by mutations in the BSS (16). Thus, both donor and branch site features appear necessary for proper splicing. Therefore, we adopted a more conservative criterion requiring an intron to exceed minimal values of both  $S_d$  and  $S_b$  for it to be classified as U12 type. Compared with *Arabidopsis* U12-type introns reported in the earlier study (3), 10 out of 11 were accurately recovered in this study, with the exception of one AT-AA intron in gene At3g51830 encoding the transmembrane protein G5p (represented by the green upside down triangle below the yellow rectangle in Fig. 1).

**Characteristics of Arabidopsis U12-dependent introns**

The identified *Arabidopsis* U12-dependent introns display patterns almost identical to the motifs of the U12-type introns

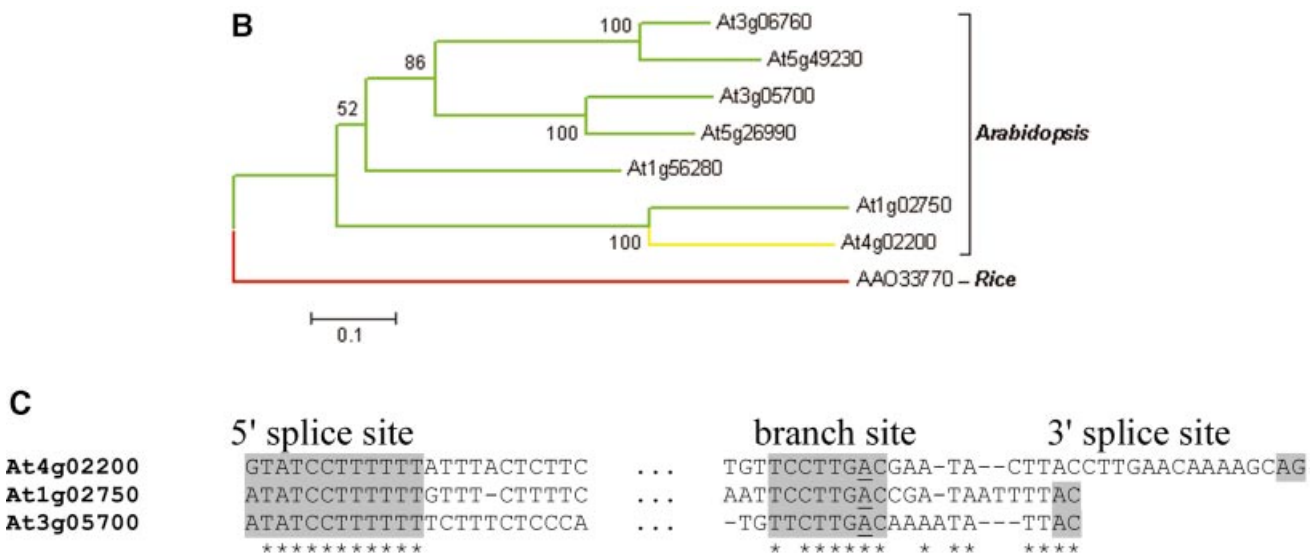


**Figure 5.** (Opposite and above) Putative drought-induced proteins. (A) Alignment of the protein sequences from *Arabidopsis* and rice. There is a phase-0 intron conservatively located immediately after the green colored column K103 in all of the genes. At that location, the rice gene AAO33770 has a U2-type GT-AG intron and the *Arabidopsis* gene At4g02200 has a U12-type GT-AG intron, whereas the remaining six genes each have a U12-type AT-AC intron. (B) Neighbor-joining tree derived from the alignment in (A). The figure scheme follows Figure 4D. (C) Alignment of the U12-type intron sequences in the genes At4g02200, At1g02750 and At3g05700. Only terminal alignments are displayed and splicing signals are indicated by shading.

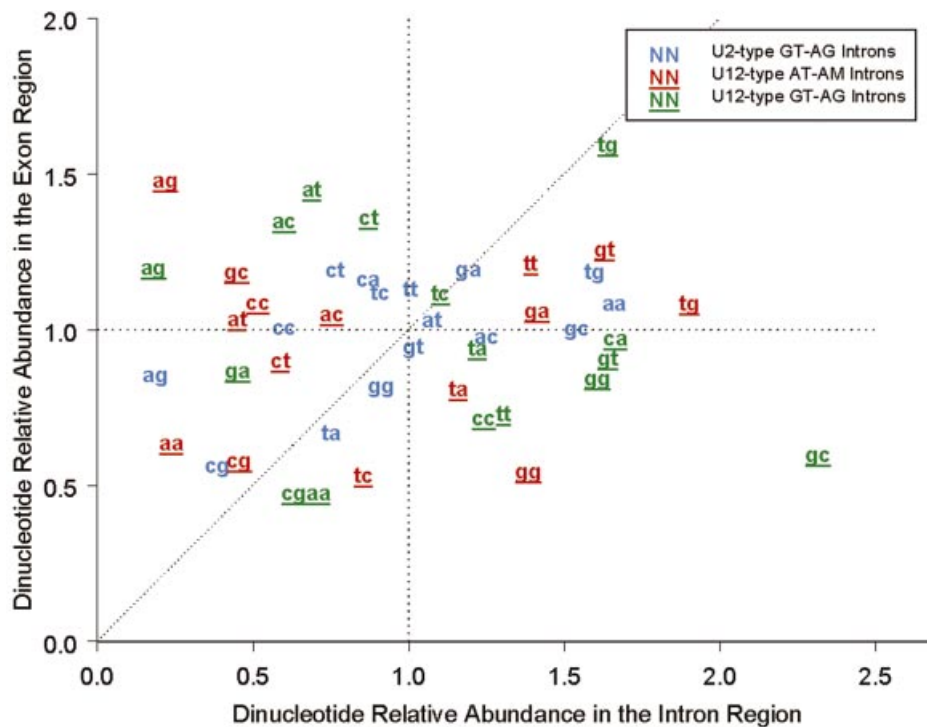


**Figure 6.** Dinucleotide relative abundances in the proximity of the 3'ss of U12- and U2-type introns. The dinucleotide relative abundances (see Materials and Methods for definition) between the BSS and the acceptor site versus the equivalent size region immediately succeeding to the acceptor site were plotted for U12-type AT-AM introns (red fonts with underline), U12-type GT-AG introns (green fonts with underline) and U2-type GT-AG introns (blue fonts).

from various other species, which is in accordance with the postulated early common origin of U12-type introns predating the divergence of animals and plants (3,19). Different from the characteristics of the U12-type introns recently identified from the human genome (14), however, our results illustrate that there is neither an appreciable difference in the distribution of intron length between U2-type introns and U12-type introns in *Arabidopsis*, nor is there a significant difference in the distribution of DistBAs between U12-type AT-AM introns and U12-type GT-AG introns (see Figs 2 and 3).

#### The distance between the branch site and the 3' splice site and the selection of the acceptor site of U12-type introns

Both of the two previous large-scale computational scans for U12-type introns were restricted to DistBA between 8 and 21 bp (3,14), based on the distribution of the DistBAs of naturally occurring U12-type introns (21). Experimental evidence for this range came mainly from the recent study of spacing mutants in the human P120 gene, in which the unfavorable dinucleotide UU with a DistBA of 12 nt was selected as the 3'ss rather than a downstream AC with a DistBA of 27 nt (23; construct +27 AC). However, the authors' conclusion that the DistBA constraint is extremely strong in U12-type intron splicing seems problematic, because the uncommon guanosine immediately prior to the +27 AC might have precluded this dinucleotide as a functional acceptor site in that construct. Here, we have made three observations that further question that conclusion, at least as a model for *Arabidopsis*. First, at least 12 U12-type introns have DistBAs larger than 21 bp, even though the mode of the

DistBA distribution is 12 nt (see Supplementary Material and Fig. 2). Secondly, only one AT-AA intron and one GT-AT intron were found in addition to the U12-dependent GT-AG and AT-AC introns, suggesting that the combination of GT-AG or AT-AC intron termini is strongly preferred in naturally occurring U12-type introns. Thirdly, there are six cases in which the dinucleotide AC is located immediately prior to the confirmed 3'ss in the U12-type AT-AC introns, indicating that the 3'ss surrounding sequence also plays an important role in the selection of the acceptor site of U12-dependent introns. Similar results were also observed in the U12-type GT-AG introns. Furthermore, the alternative 3'ss events in the U12-type GT-AG introns (Table 1) also confirm that distal acceptor sites with favorable sequence context can compete with the proximal wild-type 3'ss in U12-type intron splicing.

A caveat concerning the existence of long DistBAs is that there might be a weak BSS actually functioning downstream of the predicted BSS. Another possibility is that the introns with long DistBA (>21 bp) may actually be spliced by the U2-type spliceosome. However, there is no experimental support for either of these scenarios, and therefore it seems more reasonable to assume that a small number of U12-type introns have longer DistBAs than previously thought. To further test the allowable DistBA range, we searched for BSS also in an extended window allowing distances up to 45 nt. Only one instance was discovered with a possible longer distance (39 nt in AtNHX6), suggesting that the adopted range is reasonable.

The functional regions of U6atac and U12 snRNAs are highly conserved between human and *Arabidopsis* (20). Therefore, the longer range DistBA values observed in the *Arabidopsis* U12-type introns in this study are likely to be also

applicable to humans and other species. Hence, rescanning the genomes of humans and other organisms with an extended search region may reveal more novel U12-type introns.

### Evolutionary origins and fates of U12-type introns

To date, the fission/fusion model proposed by Burge *et al.* (3) is well accepted as an explanation of the origin of the U12-dependent spliceosome. According to this model, two splicing systems diverged in two separate lineages, but fused (probably via endosymbiosis) in a progenitor of higher eukaryotes (3). Compared with the parasitic invasion and codivergence model, the fission/fusion model provides a better explanation for the observation of genes with multiple U12-type introns (3). The analysis of Na<sup>+</sup>/H<sup>+</sup> antiporters in this study gives additional support to the fission/fusion model. There are three U12-type introns in AtNHX5–6 and HsNHE6 (and probably also in HsNHE7, if the predicted U12-type AT-AC intron is actually also spliced *in vivo*; see Fig. 4B). Two out of the three U12-type introns are conserved across human and *Arabidopsis*, and the remaining one is unrelated between each other. This implies that at least two U12-type introns in AtNHX5–6 and HsNHE6–7 have orthologous origins, and the common ancestor of AtNHX5–6 and HsNHE6–7 may have contained at least four U12-type introns. Phylogenetic analysis of the Na<sup>+</sup>/H<sup>+</sup> antiporter family dated the likely fusion event as being prior to the divergence of the plant kingdom and the animal kingdom and subsequent to the divergence of AtNHX1–4 and AtNHX5–6 [Fig. 4D; also see fig. 2 in Yokoi *et al.* (35)]. This analysis also gives the evidence that the U12-type introns are evolutionarily stable over one billion years. This amazing stability probably results from the unusual conserved U12-dependent 5'ss and BSS, so that any mutation in the splice signal sequences may easily disrupt the normal splicing of the U12-type AT-AC introns and thereby is strongly selected against. The alternative splicing examples, however, also demonstrate that U12-type AT-AC introns can be lost by intron retention, which is probably caused by mutations in the U12-dependent splice signals. In addition to the experimental evidence indicating that the U12-dependent 5'ss can be exploited by the major spliceosome (24), the alternative splicing events captured in this study also indicate that the 3'ss (probably as well as the BSS) of the U12-type GT-AG introns can also be exploited by the major spliceosome. Therefore, mutations that corrupt the conserved U12-dependent splice signals may easily trigger the conversion from the U12-type GT-AG introns to the U2-type GT-AG intron, while the reverse process is highly improbable.

Besides stability or loss, another fate of U12-type AT-AC introns may involve switching to U12-type GT-AG introns. A plausible mechanism of the switch is as follows. The 5' terminal dinucleotide /AT mutates to /GT and then the first AG or the distal AG with the favored surrounding sequence in the downstream of the BSS is selected in the U12-type intron splicing. Under this model, the mutation is likely to cause the downstream exon to be truncated or extended with an alternate reading frame. Therefore, the chance of conversion from U12-type AT-AC introns to U12-type GT-AG introns is very low. Another mechanism of the switch proposed by Burge *et al.* (3) is from AT-AC to AT-AG and then to GT-AG. However, because it requires two mutation events and the occurrence of natural AT-AG introns is extremely low, the chance of

successful conversion under this pathway should be also extremely low. At any rate, the switch between the U12-type AT-AC intron and the U12-type GT-AG intron should be much rarer than the conversion from the U12-type GT-AG intron to the U2-type GT-AG intron. However, it is difficult to explain why the U12-type GT-AG introns outnumber the U12-type AT-AC introns. We are forced to infer that U12-type GT-AG introns did not originate from U12-type AT-AC introns but appeared together with the latter one billion years ago. The analysis of the Na<sup>+</sup>/H<sup>+</sup> antiporters supports this conjecture (see Fig. 4D). However, another plausible explanation is that there is some kind of selection against the conversion from the U12-type GT-AG intron to the U2-type GT-AG intron. It was noted that most of the genes containing U12-type introns function in information processing (3). In this study, some of the genes containing U12-type introns were found to be stress reaction related, such as the putative drought-induced proteins (Fig. 5) and AtNHX5, whose expression level increases in response to salt treatment (35). It is possible that the U12-dependent spliceosome system might be activated and therefore regulates the expression level of target genes that contain U12-type introns via changing the speed of U12-type intron splicing (36) in response to stresses in plants or the analogous situations in vertebrates or insects. In this scheme, the potential role of the U12-dependent spliceosome system may result in selective pressure against the conversion from U12-type GT-AG introns to U2-type GT-AG introns.

In spite of the high stability and possible selective advantage, it is likely that the number of U12-type introns has been slowly but continuously reduced by accumulating mutations. Gene duplication, however, may help the U12-type introns propagate within the gene families, for example, the putative drought-induced protein family, Na<sup>+</sup>/H<sup>+</sup> antiporters and dTDP-glucose 4-6-dehydratase like proteins (26).

### SUPPLEMENTARY MATERIAL

Supplementary Material is available at NAR Online.

### ACKNOWLEDGEMENTS

The authors would like to thank Jacqueline E. Townsend for help with preparation of the manuscript, Richard A. Padgett for kindly providing reprints, and Shannon D. Schlueter for critical discussions. This work was supported in part by NSF grant DBI-0110254 to V.B.

### REFERENCES

1. Jackson, I.J. (1991) A reappraisal of non-consensus mRNA splice sites. *Nucleic Acids Res.*, **19**, 3795–3798.
2. Hall, S.L. and Padgett, R.A. (1994) Conserved sequences in a class of rare eukaryotic nuclear introns with non-consensus splice sites. *J. Mol. Biol.*, **239**, 357–365.
3. Burge, C.B., Padgett, R.A. and Sharp, P.A. (1998) Evolutionary fates and origins of U12-type introns. *Mol. Cell*, **2**, 773–785.
4. Burge, C.B., Tuschl, T. and Sharp, P.A. (1999) Splicing of precursors to mRNAs by the spliceosomes. In Gesteland, R.F., Cech, T. and Atkins, J.F. (eds), *The RNA World II*. Cold Spring Harbor Laboratory Press, Cold Spring Harbor, NY, pp. 525–560.
5. Wu, Q. and Krainer, A.R. (1999) AT-AC pre-mRNA splicing mechanisms and conservation of minor introns in voltage-gated ion channel genes. *Mol. Cell. Biol.*, **19**, 3225–3236.

6. Hall, S.L. and Padgett, R.A. (1996) Requirement of U12 snRNA for *in vivo* splicing of a minor class of eukaryotic nuclear pre-mRNA introns. *Science*, **271**, 1716–1718.
7. Tarn, W.Y. and Steitz, J.A. (1996) Highly diverged U4 and U6 small nuclear RNAs required for splicing rare AT-AC introns. *Science*, **273**, 1824–1832.
8. Tarn, W.Y. and Steitz, J.A. (1996) A novel spliceosome containing U11, U12 and U5 snRNPs excises a minor class (AT-AC) intron *in vitro*. *Cell*, **84**, 801–811.
9. Shukla, G.C. and Padgett, R.A. (2001) The intramolecular stem-loop structure of U6 snRNA can functionally replace the U6atac snRNA stem-loop. *RNA*, **7**, 94–105.
10. Luo, H.R., Moreau, G.A., Levin, N. and Moore, M.J. (1999) The human Prp8 protein is a component of both U2- and U12-dependent spliceosomes. *RNA*, **5**, 893–908.
11. Will, C.L., Schneider, C., Reed, R. and Lührmann, R. (1999) Identification of both shared and distinct proteins in the major and minor spliceosomes. *Science*, **284**, 2003–2005.
12. Will, C.L., Schneider, C., MacMillan, A.M., Katopodis, N.F., Neubauer, G., Wilm, M., Lührmann, R. and Query, C.C. (2001) A novel U2 and U11/U12 snRNP protein that associates with the pre-mRNA branch site. *EMBO J.*, **20**, 4536–4546.
13. Schneider, C., Will, C.L., Makarova, O.V., Makarov, E.M. and Lührmann, R. (2002) Human U4/U6.U5 and U4atac/U6atac.U5 tri-snRNPs exhibit similar protein compositions. *Mol. Cell Biol.*, **22**, 3219–3229.
14. Levine, A. and Durbin, R. (2001) A computational scan for U12-dependent introns in the human genome sequence. *Nucleic Acids Res.*, **29**, 4006–4013.
15. Wu, Q. and Krainer, A.R. (1996) U1-mediated exon definition interactions between AT-AC and GT-AG introns. *Science*, **274**, 1005–1008.
16. Dietrich, R.C., Shukla, G.C., Fuller, J.D. and Padgett, R.A. (2001) Alternative splicing of U12-dependent introns *in vivo* responds to purine-rich enhancers. *RNA*, **7**, 1378–1388.
17. Hastings, M.L. and Krainer, A.R. (2001) Functions of SR proteins in the U12-dependent AT-AC pre-mRNA splicing pathway. *RNA*, **7**, 471–482.
18. Frilander, M.J. and Steitz, J.A. (1999) Initial recognition of U12-dependent introns requires both U11/5' splice-site and U12/branchpoint interactions. *Genes Dev.*, **13**, 851–863.
19. Wu, H.J., Gaubier-Comella, P., Delseny, M., Grellet, F., Van Montagu, M. and Rouzé, P. (1996) Non-canonical introns are at least 10<sup>9</sup> years old. *Nature Genet.*, **14**, 383–384.
20. Shukla, G.C. and Padgett, R.A. (1999) Conservation of functional features of U6atac and U12 snRNAs between vertebrates and higher plants. *RNA*, **5**, 525–538.
21. Sharp, P.A. and Burge, C.B. (1997) Classification of introns: U2-type or U12-type. *Cell*, **91**, 875–879.
22. Smith, C.W. and Nadal-Ginard, B. (1989) Mutually exclusive splicing of alpha-tropomyosin exons enforced by an unusual lariat branch point location: implications for constitutive splicing. *Cell*, **56**, 749–758.
23. Dietrich, R.C., Peris, M.J., Seyboldt, A.S. and Padgett, R.A. (2001) Role of the 3' splice site in U12-dependent intron splicing. *Mol. Cell Biol.*, **21**, 1942–1952.
24. Dietrich, R.C., Incorvaia, R. and Padgett, R.A. (1997) Terminal intron dinucleotide sequences do not distinguish between U2- and U12-dependent introns. *Mol. Cell*, **1**, 151–160.
25. Wu, Q. and Krainer, A.R. (1997) Splicing of a divergent subclass of AT-AC introns requires the major spliceosomal snRNAs. *RNA*, **3**, 586–601.
26. Zhu, W., Schlueter, S.H. and Brendel, V. (2003) Refined annotation of the *Arabidopsis* genome by complete expressed sequence tag mapping. *Plant Physiol.*, **132**, 469–484.
27. Usuka, J., Zhu, W. and Brendel, V. (2000) Optimal spliced alignment of homologous cDNA to a genomic DNA template. *Bioinformatics*, **16**, 203–211.
28. Bailey, T.L. and Elkan, C. (1994) Fitting a mixture model by expectation maximization to discover motifs in biopolymers. *Proc. Int. Conf. Intell. Syst. Mol. Biol.*, **2**, 28–36.
29. Blanc, G., Hokamp, K. and Wolfe, K.H. (2003) A recent polyploidy superimposed on older large-scale duplications in the *Arabidopsis* genome. *Genome Res.*, **13**, 137–144.
30. Jeanmougin, F., Thompson, J.D., Gouy, M., Higgins, D.G. and Gibson, T.J. (1998) Multiple sequence alignment with Clustal X. *Trends Biochem. Sci.*, **23**, 403–405.
31. Kumar, S., Tamura, K., Jakobsen, I.B. and Nei, M. (2001) MEGA2: molecular evolutionary genetics analysis software. *Bioinformatics*, **17**, 1244–1245.
32. Burge, C., Campbell, A.M. and Karlin, S. (1992) Over- and under-representation of short oligonucleotides in DNA sequences. *Proc. Natl Acad. Sci. USA*, **89**, 1358–1362.
33. Brendel, V., Carle-Urioste, J.C. and Walbot, V. (1998) Intron recognition in plants. In Bailey-Serres, J. and Gallie, D.R. (eds), *A Look Beyond Transcription: Mechanisms Determining mRNA Stability and Translation in Plants*. American Society of Plant Physiology, Rockville, MD, USA, pp. 20–28.
34. Altschul, S.F., Madden, T.L., Schaffer, A.A., Zhang, J., Zhang, Z., Miller, W. and Lipman, D.J. (1997) Gapped BLAST and PSI-BLAST: a new generation of protein database search programs. *Nucleic Acids Res.*, **25**, 3389–3402.
35. Yokoi, S., Quintero, F.J., Cubero, B., Ruiz, M.T., Bressan, R.A., Hasegawa, P.M. and Pardo, J.M. (2002) Differential expression and function of *Arabidopsis thaliana* NHX Na<sup>+</sup>/H<sup>+</sup> antiporters in the salt stress response. *Plant J.*, **30**, 529–539.
36. Patel, A.A., McCarthy, M. and Steitz, J.A. (2002) The splicing of U12-type introns can be a rate-limiting step in gene expression. *EMBO J.*, **21**, 3804–3815.